Fermi National Accelerator Laboratory

FERMILAB-PUB-94/135-T
NUHEP-TH-94-11
OCIP/C-94-3
hep-ph/9405407
May 1994

Fragmentation production of J/ψ and ψ' at the Tevatron

Eric Braaten[1]
Fermi National Accelerator Laboratory, P.O. Box 500, Batavia, IL 60510

Michael A. Doncheski
Department of Physics, Carleton University, Ottawa, Ontario K1S 5B6, Canada

Sean Fleming
Department of Physics and Astronomy, Northwestern University, Evanston, IL 60208

Michelangelo L. Mangano[2]
INFN, Scuola Normale Superiore and Dipartimento di Fisica, Pisa, Italy

Abstract

We present a calculation of the charm and gluon fragmentation contributions to inclusive J/ψ and ψ' production at large transverse momentum at the Tevatron. For ψ production, we include both fragmentation directly into ψ and fragmentation into χ_c followed by the radiative decay $\chi_c \to \psi+\gamma$. We find that fragmentation overwhelms the leading-order mechanisms for prompt ψ production at large p_T, and that the dominant contributions come from fragmentation into χ_c. Our results are consistent with recent data on ψ production from the CDF and D0 experiments. In the case of prompt ψ' production, the dominant mechanism at large p_T is charm fragmentation into ψ'. We find serious disagreement between our theoretical predictions and recent ψ' data from the Tevatron.

[1]On leave from the Dept. of Physics and Astronomy, Northwestern University, Evanston, IL 60208
[2]Address after Febr. 1, 1995: CERN, TH Division, Geneva, Switzerland.

Operated by Universities Research Association Inc. under contract with the United States Department of Energy

1 Introduction

The study of charmonium production in high energy hadronic collisions provides an important testing ground for perturbative quantum chromodynamics (QCD). The J/ψ and ψ' states are of particular interest since they are produced in abundance and are relatively easy to detect at a collider such as the Tevatron. In earlier calculations of direct charmonium production at large transverse momentum (p_T) in $p\bar{p}$ collisions [1] , it was assumed that the leading-order diagrams give the dominant contributions to the cross section. These calculations did not reproduce all aspects of the available data [2, 3, 4], suggesting that there are other important production mechanisms. It was pointed out by Braaten and Yuan [5] in 1993 that fragmentation processes, while formally of higher order in the strong coupling constant α_s, will dominate at sufficiently large p_T. Explicit calculations of the contribution to ψ production at the Tevatron from the fragmentation of gluons and charm quarks revealed that fragmentation dominates over the leading-order gluon-gluon fusion mechanism for p_T greater than about 6 GeV [6]. In addition to being directly produced, the ψ signal is also fed by the χ_c states through the radiative decay $\chi_c \to \psi + \gamma$. In this paper, we present more complete calculations for ψ production, including the effects of χ_c's that are produced by fragmentation, and compare the results with recent data on prompt and inclusive ψ production from the CDF and D0 experiments. We also compare our calculations of ψ' production with recent data from CDF.

While this paper was being written, similar work on ψ-production was presented in a paper by Cacciari and Greco [7].

2 Fragmentation Formalism

Factorization theorems of perturbative QCD indicate that the inclusive production of a hadron at large p_T is dominated by fragmentation. Fragmentation is the production of a parton with large transverse momentum which subsequently forms a jet containing the desired hadron. In the case of $p\bar{p}$ collisions, the fragmentation contribution to the cross section can be expressed as a convolution of parton distribution functions, hard-scattering cross sections, and fragmentation functions. Taking ψ production to be specific, the differential

cross section can be written as:

$$d\sigma(p\bar{p} \to \psi(p_T, y) + X) = \sum_i \int_0^1 dz\; d\sigma(p\bar{p} \to i(\frac{p_T}{z}, y) + X, {\mu_{\rm frag}}^2)\; D_{i\to\psi}(z, {\mu_{\rm frag}}^2), \qquad (1)$$

where z is the longitudinal momentum fraction of the ψ relative to parton i, y is the rapidity of the ψ, and $D_{i\to\psi}(z, {\mu_{\rm frag}}^2)$ is the fragmentation function. The dependence on the fragmentation scale $\mu_{\rm frag}$ cancels between the two factors only after inclusion of all orders of the perturbative expansion. The differential cross section on the right side of (1) can in turn be written as the convolution of parton distributions $f_{j/p}$ and $f_{k/\bar{p}}$ in the proton and antiproton with hard-scattering differential cross sections $d\hat{\sigma}$ for the parton subprocesses $j + k \to i + X$. In low-order calculations, the fragmentation scale $\mu_{\rm frag}$, the factorization scale $\mu_{\rm F}$, and the renormalization scale $\mu_{\rm R}$ should all be chosen on the order of p_T/z, the transverse momentum of the fragmenting parton. The dominant contributions to Eq. (1) come from gluon fragmentation and charm fragmentation. Fragmentation of light quarks will only contribute at low z, and is therefore strongly suppressed by the rapidly falling p_T spectrum of the final-state partons from the hard-scattering process. The inclusive ψ signal is also fed by production of the P-wave χ_c states followed by the radiative decay $\chi_c \to \psi + \gamma$. The fragmentation contributions can be obtained by multiplying the χ_c production cross sections analogous to (1) by the radiative branching fractions 0.007, 0.27, and 0.135 for χ_{c0}, χ_{c1}, and χ_{c2}, respectively.

The fragmentation functions $D(z)$ for charmonium production can be calculated within perturbative QCD [5, 8]. The relevant fragmentation functions for the production of the S-wave and P-wave states have all been calculated to leading order in α_s. In this paper we use the fragmentation functions for $g \to \psi$ [5], $c \to \psi$ [10], $g \to \chi_c$ [11], $c \to \chi_c$ [12], and $\gamma \to \psi$ [13]. The perturbative calculations give the fragmentation functions at an initial scale μ_0 of order m_c. We take this initial scale to be $\mu_0 = 2m_c$ for gluon and photon fragmentation, and $\mu_0 = 3m_c$ for charm fragmentation. The fragmentation functions are then evolved up to the scale $\mu_{\rm frag} = \mathcal{O}p_T/z$ set by the transverse momentum of the fragmenting parton using the Altarelli-Parisi evolution equations:

$$\mu^2 \frac{\partial}{\partial \mu^2} D_{i\to\psi}(z, \mu^2) = \frac{\alpha_s}{2\pi} \sum_j \int_z^1 \frac{dy}{y}\; P_{ij}(z/y)\; D_{j\to\psi}(y, \mu^2). \qquad (2)$$

We included in Eq. (2) only the P_{gg} splitting term for gluon fragmentation and only the P_{cc} term for charm fragmentation. With the exception of $D_{g\to\psi}$, the inclusion of the off-diagonal Altarelli-Parisi kernels would give corrections that are safely negligible within the accuracy of a leading-order (LO) calculation. In the case of $D_{g\to\psi}$, the P_{gc} term in (2) is important because the initial fragmentation function $D_{c\to\psi}(z,\mu_0^2)$ is more than an order of magnitude larger than $D_{g\to\psi}(z,\mu_0^2)$ [9]. In the present analysis, we take this effect into account by including the next-to-leading-order (NLO) corrections to the hard-scattering cross sections $d\hat{\sigma}$ for inclusive charm production [14]. These higher order terms include the numerically important contributions from final state gluon splitting into $c\bar{c}$ pairs. Having included this effect in the hard-scattering cross sections, we do not have to account for them via the $g \to c\bar{c}$ Altarelli-Parisi kernel as in Ref. [7]. Higher-order terms from off-diagonal Altarelli-Parisi evolution, such as $g \to c\bar{c}$ splitting from secondary gluons in the gluon-jet cascade, contribute to the overall charmonium multiplicity inside the jet, but the enhancement comes only in the small z region and it can therefore be safely neglected in the LO p_T distribution.

We now discuss the uncertainties in the calculations of the fragmentation contribution to the differential cross section for charmonium production. We first consider the initial fragmentation functions $D(z,\mu_0^2)$. They have been calculated only to leading order in α_s and to leading order in a nonrelativistic expansion. Based on the NLO calculations of the annihilation rates for charmonium, we anticipate that NLO corrections to the fragmentation functions may be as large as 50%. A rough estimate of the size of relativistic corrections is the average value of v^2/c^2 in potential models, which is about 30%. The normalizations of the initial fragmentation functions are calculated in terms of α_s, m_c, and various nonperturbative matrix elements. For the charm quark mass, we use the value $m_c = 1.5$ GeV. While m_c appears in the fragmentation functions raised to the third or fifth power, this is not a large source of uncertainty since roughly the same power appears in the quantities that are used to determine the nonperturbative matrix elements. The S-wave fragmentation functions depend on the wavefunction at the origin, which we take to be $|R_\psi(0)|^2 = 0.7$ GeV^3. This value is obtained from the electronic width of the ψ, including the effect of the NLO perturbative correction, which is about 50%, but not taking into account relativistic corrections. The P-wave fragmentation functions depend on two nonperturbative parameters. For the

derivative of the radial wavefunction at the origin, we use the value $|R'_{\chi_c}(0)|^2 = 0.053$ GeV^5. This value is determined from the annihilation rates of the χ_c states [15], neglecting the as-yet-uncalculated NLO perturbative corrections as well as relativistic corrections. The least well-determined parameter in the P-wave fragmentation functions is a parameter H'_8 associated with the color-octet mechanism for P-wave production [16]. This parameter is poorly constrained, lying in the range $2.2 < H'_8 < 25$ MeV [11, 17]. We use the value $H'_8 = 3$ MeV, which is consistent with measured branching fractions for B mesons into the χ_c states [16].

We next consider errors due to the evolution of the fragmentation functions from the initial scale μ_0 up to the scale p_T/z. The Altarelli-Parisi equations Eq. (2) break down in the small-z region, due to large logarithms of $1/z$ in the perturbation expansion. The most dramatic effect of this breakdown is an unphysical divergence in the gluon multiplicity at low momentum fraction [18]. This leads to a correspondingly large overestimate of the gluon fragmentation functions into charmonium at small values of z. We do not expect this to be a serious problem at the values of p_T considered in this paper, because the cross sections are dominated by larger values of z due to the steeply falling spectrum of the hard partons. We find empirically that the Monte Carlo calculations presented below rarely sampled values of z smaller than 0.1.

While the divergence of the gluon multiplicity at small z may not in itself be a problem, it is a symptom of a deficiency of Altarelli-Parisi evolution that also has consequences at larger values of z. In particular, the naive Altarelli-Parisi equations do not respect the phase-space constraint $D_{g\to\psi}(z,\mu^2) = 0$ for $z < M_\psi^2/\mu^2$. The implementation of this constraint would slow down the evolution of the fragmentation function by delaying the depletion of the large-z fragmentation region. Since the spectrum of gluons and charm quarks falls rapidly with p_T/z, a proper treatment of the large-z region can have a significant effect on the cross section. A more accurate treatment would be to use the following system of equations for the evolution of the gluon fragmentation functions:

$$D(z,\mu^2) = \int_{M_\psi^2}^{\mu^2} \frac{dq^2}{q^2} \int_z^1 \frac{dy}{y} G(y,q^2;\mu^2) d(z/y,q^2) \tag{3}$$

$$\mu^2 \frac{\partial}{\partial \mu^2} G(z,\mu^2;\mu_0^2) = \frac{\alpha_s}{2\pi} \int_z^1 \frac{dy}{y} P_{gg}(y)\, G(z/y,\mu^2;y\mu_0^2) \tag{4}$$

where $G(z,\mu^2;\mu_0^2)$ is the distribution of gluons of virtuality μ inside a gluon of virtuality μ_0, which is subject to the boundary condition $G(z,\mu_0^2;\mu_0^2) = \delta(1-z)$. The function $d(z,q^2)$ [5] is the LO probability that a gluon of virtuality q decays to a ψ carrying longitudinal momentum fraction z in the infinite momentum frame. The initial fragmentation functions in our present treatment are given by $D(z,\mu_0^2) = \int_0^\infty (ds/s) d(z,s)$. The system of equations (3) and (4) gives the correct ψ multiplicity inside a gluon jet [19], after inclusion of small-z coherence effects [18]. It is straightforward to show that this system is equivalent to the following nonhomogeneous evolution equation:

$$\mu^2 \frac{\partial}{\partial \mu^2} D(z,\mu^2) \;=\; d(z,\mu^2) \;+\; \frac{\alpha_s}{2\pi} \int_z^1 \frac{dy}{y}\; P_{gg}(y)\; D(z/y, y\mu^2), \tag{5}$$

together with the boundary condition $D(y,\mu^2 = M_\psi^2) = 0$. This evolution equation respects the phase space constraint, as can be easily checked [18]. A thorough study of this generalized evolution equation and its consequences for charmonium production will be presented elsewhere.

The evolution equation presented above also solves a problem involving threshold effects in our fragmentation functions. The p_T values for which the fragmentation contributions become important are, in fact, too small to be considered in the asymptotic regime where threshold effects can be ignored. In the calculations of the initial fragmentation functions $D(z,\mu_0^2)$, the assumption $\mu_0^2 \gg 4m_c^2/z$ was used to obtain simple analytic results. This assumption is not really compatible with the subsequent identification $\mu_0 = 2m_c$. The resulting error may be negligible after evolution to asymptotically large μ, but it is probably significant at the scales needed in our calculations. The evolution equation (5) treats threshold effects consistently. In the present analysis, we estimate the error due to our treatment of threshold effects by determining the change in the cross section that results from increasing the value of μ_0 by a factor of 2.

There are several other sources of uncertainty. The uncertainties due to the choice of the renormalization scale, the factorization scale, and the fragmentation scale can be estimated by varying these scales by factors of 2. The error from the parton distributions can be estimated by repeating the calculations using different parton distributions. Another source of error at small p_T is the neglect of the intrinsic transverse momentum of the partons

in the proton and antiproton [20, 21]. The effect of the intrinsic transverse momentum is most significant for partons with very small longitudinal momentum fraction x. It should not be important at large p_T because ψ production at large p_T does not probe deeply into the small-x region of the parton distribution. Finally there is the NLO perturbative correction to the hard-scattering cross section $d\hat{\sigma}$, which we only included in the case of charm fragmentation. The NLO corrections to the gluon p_T spectrum have been evaluated in ref. [7] , where it was shown that they increase the rate for χ production from fragmentation by about 50%. Needless to say, a full NLO calculation of both the hard-scattering cross sections and the fragmentation functions would be highly nontrivial.

Considering all the uncertainties discussed above, we believe that the error in our fragmentation calculations can easily be larger than a factor of 2, but it is definitely less than an order of magnitude. One should of course keep in mind that in addition to fragmentation, which must dominate at sufficiently large p_T, there are other contributions suppressed by factors of m_c^2/p_T^2 that may be important at the values of p_T that are available experimentally.

3 Results and discussion

In figure 1 we plot the individual contributions to the differential cross section for prompt ψ production as a function of p_T. We include results for both the fragmentation contributions and the leading-order contributions[2]. Note that each of the χ_c production curves is a sum over the three P-wave states χ_{c0}, χ_{c1}, and χ_{c2}. We used the MRSD0 parton distribution set, and chose the renormalization ($\mu_{\rm R}$), factorization ($\mu_{\rm F}$) and fragmentation ($\mu_{\rm frag}$) scales to be same, and equal to the transverse momentum of the fragmenting parton, P_T=p_T/z. In order to compare with available data from the Tevatron, we imposed a pseudorapidity cut of $|\eta| < 0.6$ on the ψ. It is evident from the graph that fragmentation dominates over the leading-order mechanisms for all values of p_T for which the fragmentation approximation is reasonable, namely for p_T greater than about 5 GeV. The dominant production mechanism by an order of magnitude is gluon fragmentation into χ_c followed by its decay into ψ. Note that, aside from photon fragmentation which is dominated by quark-gluon initial states, all the

[2]The results for direct ψ inclusive p_T distributions given in ref. [4] are incorrect, due to a coding error in the choice of $\mu_{\rm R}$ and $\mu_{\rm F}$.

fragmentation contributions have the same p_T-dependence. The leading-order χ_c production falls off more rapidly with p_T, and that leading-order ψ production falls off still more rapidly. This pattern simply reflects the p_T-dependence of the underlying hard-scattering processes: $d\hat{\sigma}/dp_T^2$ scales like $1/p_T^4$ for fragmentation, $1/p_T^6$ for leading-order χ_c production, and $1/p_T^8$ for leading-order ψ production.

In figure 2, the sum of the fragmentation contributions (two solid curves) and the sum of the leading-order contributions (two dashed curves) are compared with preliminary CDF data for prompt ψ production [22]. The contribution to ψ production from b-hadron decays has been removed from the data via detection of the secondary vertex from which the ψ's originate [22]. The upper and lower curves in figure 3 were obtained by varying the scales μ_R, μ_F and μ_{frag} used in the calculation, in order to provide an estimate of the systematic uncertainty associated with the LO calculation. The upper curve corresponds to $\mu_R=\mu_F=P_T/2$ and $\mu_{frag}=\max(P_T/2,\mu_0)$, while the lower curve is obtained for $\mu_R=\mu_F=\mu_{frag}=2P_T$. The cross-over of the curves at small p_T is due to the rapid growth of the parton distribution functions with increasing scale, and should be considered an artificial reduction of scale sensitivity. The errors from varying the parton distributions are only about 10%. We estimate the error from threshold effects in the fragmentation functions by increasing μ_0 by a factor of 2. The effect of this is a decrease of the fragmentation contribution, by a factor of 2, at $p_T = 3$ GeV, and an increase, by a factor of 2, at $p_T = 20$ GeV. Another large uncertainty comes from the color-octet parameter H_8' in the fragmentation functions for $g \to \chi_c$. Changing H_8' by a factor of two changes our results by a factor of 2 at the largest p_T available. While the shapes of the leading-order curve and the fragmentation curve are both consistent with the data over the range of p_T that is available, the normalization of the leading-order contribution is too small by more than an order of magnitude. The fragmentation contribution has the correct normalization to within a factor of 2 or 3, which can be easily accounted for by the uncertainties discussed above. We conclude that the fragmentation calculation is not inconsistent with the CDF data on prompt ψ production.

We also present in fig. 3 a comparison of the theoretical predictions for fully inclusive ψ production (including those from b-hadron decays) with data from CDF [22] and D0 [23]. The theoretical contribution from b-decays used here was evaluated at NLO as in Ref. [4].

The predictions are consistent with the data.

We next consider the production of ψ', which should not receive any contributions from higher charmonium states. The ψ' fragmentation contribution can be obtained from the $g \to \psi$, $c \to \psi$, and $\gamma \to \psi$ fragmentation contribution simply by multiplying by the ratio of the electronic widths of the ψ' and ψ. The total fragmentation contribution (two solid curves) and the leading-order contribution (two dashed curves) are shown in figure 4, along with the preliminary CDF data [24]. Again the contribution from b–hadron decays has been subtracted using the secondary vertex information. The pairs of curves correspond to the same choices of scales as in figure 2. The dominant production mechanisms are gluon-gluon fusion for p_T below about 5 GeV, and charm quark fragmentation into ψ' for larger p_T. The leading-order curve falls much too rapidly with p_T to explain the data, but the fragmentation curve has the correct shape. However, in striking contrast to the case of ψ production, the normalization of the fragmentation contribution to ψ' production is too small by more than an order of magnitude. That there is such a large discrepancy between theory and experiment in the case of ψ', but not for ψ, is extremely interesting. It suggests that there are other important mechanisms for production of S-wave states at large p_T beyond those that have presently been calculated. While such processes would certainly affect ψ production as well, their effect may not be as dramatic because of the large contribution from χ_c-production in the case of the ψ.

One possible such mechanism is the process $gg \to \psi gg$, with a gluon exchanged in the t-channel. This is a subset of the NLO corrections to the process $gg \to \psi g$ for which the hard-scattering cross section has a p_T-dependence that is intermediate between the leading-order diagrams and the fragmentation contribution. It is easy to verify that $d\hat{\sigma}/dp_T^2$ for this process scales asymptotically like ${\alpha_s}^4/{p_T}^6$, compared to ${\alpha_s}^3/{p_T}^8$ for $gg \to \psi g$ and compared to ${\alpha_s}^5/{p_T}^4$ for the NNLO correction, which includes gluon fragmentation. The shape of the p_T distribution from this process should be similar to that for leading-order χ_c production, which is compatible with the data. Whether the normalization agrees can only be determined by explicit calculation. Such a calculation is in progress.

Note that, like the decay of a b-hadron, the fragmentation mechanism produces ψ's inside a jet of light hadrons. A nonisolation cut on the ψ can therefore not be used to tag

ψ's coming from B meson decay. One might hope that an isolation cut could be used to separate prompt ψ's produced by the leading-order mechanisms from those produced by fragmentation. However, we found in our calculations that the average value of z for a ψ produced by fragmentation is $\langle z \rangle = 0.7$. This means that the remaining partons in the jet containing the ψ share on average less than 1/2 the energy of the ψ, and thus may often be too soft to be detected reliably.

4 Conclusion

We have calculated the cross section for production of prompt ψ at large p_T at the Tevatron including the effects of gluon and charm fragmentation. The largest contributions by an order of magnitude come from gluon fragmentation into χ_c, followed by the decay $\chi_c \to \psi + \gamma$. The results of this calculation are not inconsistent with preliminary CDF data, given the uncertainties in the fragmentation functions. In contrast, the leading-order mechanisms give a result that is nearly an order of magnitude too small.

We have also calculated inclusive ψ' production at large p_T at the Tevatron. We find that fragmentation dominates for p_T greater than about 6 GeV, with the largest contribution coming from charm fragmentation into ψ'. Comparing the results of the calculation to preliminary CDF data, we find that the cross section is too small by more than an order of magnitude, even after including the fragmentation mechanism. Thus while the fragmentation mechanism may provide an explanation for the observed rate of prompt ψ production at large p_T, it does not seem to explain the existing data for ψ'. We discussed the possibility of additional mechanisms for charmonium production at large p_T beyond those that have presently been calculated. Furthermore, we discussed some of the intrinsic theoretical uncertainties present in these calculations and anticipated some studies that can be undertaken to improve the present theoretical framework.

The work of M.A.D. is supported in part by the Natural Sciences and Engineering Research Council of Canada through a Canada International Fellowship. The work of M.L.M. is supported in part by the EEC Programme "Human Capital and Mobility", Network "Physics at High Energy Colliders", contract CHRX-CT93-0537 (DG 12 COMA). The work

of E.B. and S.F. was supported in part by the U.S. Department of Energy, Division of High Energy Physics, under Grant DE-FG02-91-ER40684. E.B. would like to thank the Fermilab theory group for their hospitality while this work was being carried out.

References

[1] R. Baier and R. Rückl, *Z. Phys.* **C19** (1983) 251; F. Halzen, F. Herzog, E.W.N. Glover, and A.D. Martin, *Phys. Rev.* **D30** (1984) 700; B. van Eijk and R. Kinnunen, *Z. Phys.* **C41** (1988) 489; E.W.N. Glover, A.D. Martin, W.J. Stirling, *Z. Phys.* **C38** (1988) 473.

[2] C. Albajar et al., UA1 Coll., *Phys. Lett.* **256B** (1991) 112.

[3] F. Abe et al., CDF Coll., *Phys. Rev. Lett.* **69** (1992) 3704.

[4] M. L. Mangano, *Z. Phys.* **C58** (1993) 651.

[5] E. Braaten and T.C. Yuan, *Phys. Rev. Lett.* **71** (1993) 1673.

[6] M.A. Doncheski, S. Fleming and M.L. Mangano, Proceedings of the Workshop on Physics at Current Accelerators and the Supercollider, FERMILAB-CONF-93/348-T (1993).

[7] M. Cacciari and M. Greco, INFN preprint, FNT/T-94/13, hep-ph/9405241.

[8] C.-H. Chang and Y.-Q. Chen, *Phys. Lett.* **B284** (1991) 127; *Phys. Rev.* **D46** (1992) 3845.

[9] A.F. Falk, M. Luke, M.J. Savage, and M.B. Wise, *Phys. Lett.* **B312** (1993) 486.

[10] E. Braaten, K. Cheung, T.C. Yuan, *Phys. Rev.* **D48** (1993) 4230.

[11] E. Braaten and T.C. Yuan, Fermilab preprint FERMILAB-PUB-94/040-T (1994).

[12] T.C. Yuan, U.C. Davis preprint UCD-94-2 (1994).

[13] S. Fleming, Fermilab preprint FERMILAB-PUB-94/074-T (1994).

[14] P. Nason, S. Dawson and R. K. Ellis, *Nucl. Phys.* **B327** (1988) 49 ; W. Beenakker et al., *Nucl. Phys.* **B351** (1991) 507.

[15] G.T. Bodwin, E. Braaten, and G.P. Lepage, *Phys. Rev.* **D46** (1992) 1914.

[16] G.T. Bodwin, E. Braaten, G.P. Lepage, and T.C. Yuan, *Phys. Rev.* **D46** (1992) R3703.

[17] H. Trottier, *Phys. Lett.* **B320** (1994) 145.

[18] A. Bassetto, M. Ciafaloni and G. Marchesini, *Phys. Rep.* **100** (1983) 201, and references therein.

[19] M.L. Mangano and P. Nason, *Phys. Lett.* **B285** (1992) 160.

[20] J.C. Collins and R.K. Ellis, *Nucl. Phys.* **B360** (1991) 3; S. Catani, M. Ciafaloni and F. Hautmann, *Nucl. Phys.* **B366** (1991) 135; E.M. Levin, M.G. Ryskin and Yu.M.

Shabelsky, *Phys. Lett.* **260B** (1991) 429.

[21] S. Catani, E. D'Emilio and L. Trentadue, *Phys. Lett.* **211B** (1988) 335.

[22] V. Papadimitriou, CDF Coll., presented at the "Rencontres de la Vallee d'Aoste", La Thuile, March 1994.

[23] K. Bazizi, D0 Coll., presented at the Rencontres de Moriond, Meribel, March 19–26 1994.

[24] T. Daniels, CDF Coll., Fermilab-Conf-94/136-E.

Figure Captions

1. Contributions to the differential cross section for inclusive ψ production at the Tevatron: fragmentation into ψ (solid curves), and the leading order contributions (dashed curves).

2. Preliminary CDF data for prompt ψ production (O) compared with theoretical predictions of the total fragmentation contribution (solid curves) and the total leading-order contribution (dashed curves).

3. Total ψ production: CDF (O) and D0 ($\diamond$) data compared to theoretical curves for prompt ψ production (solid curves), and theoretical predictions for b-hadron decays (dashed curves).

4. Preliminary CDF data for prompt ψ' production (O) compared with theoretical predictions of the total fragmentation contribution (solid curves) and the total leading-order contribution (dashed curves).

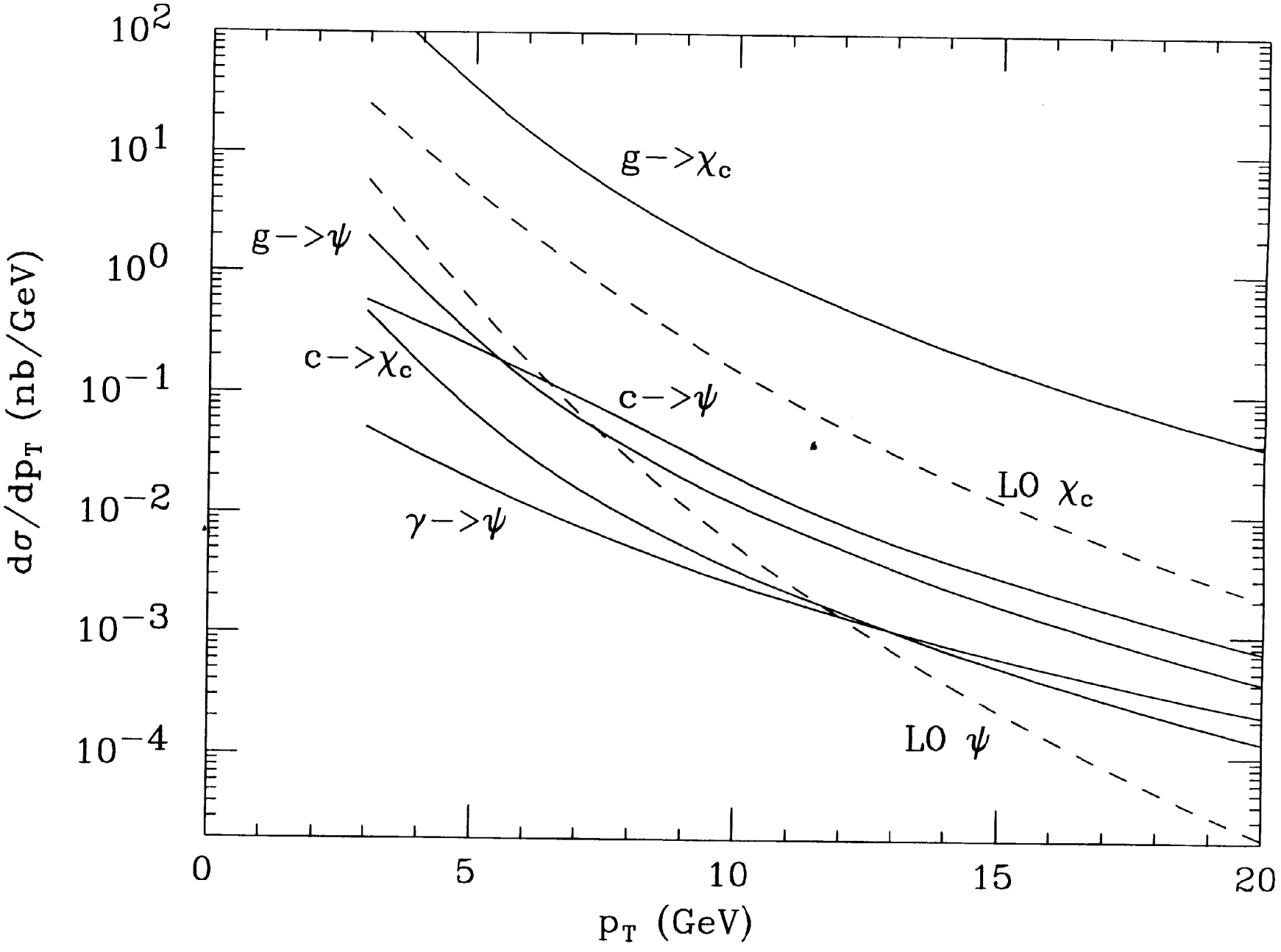
10^2
10^1
10^0
10^{-1}
10^{-2}
10^{-3}
10^{-4}
$d\sigma/dp_T$ (nb/GeV)
g->χ_c
g->ψ
c->χ_c
c->ψ
γ->ψ
LO χ_c
LO ψ
0
5
10
15
20
p_T (GeV)

Figure 1

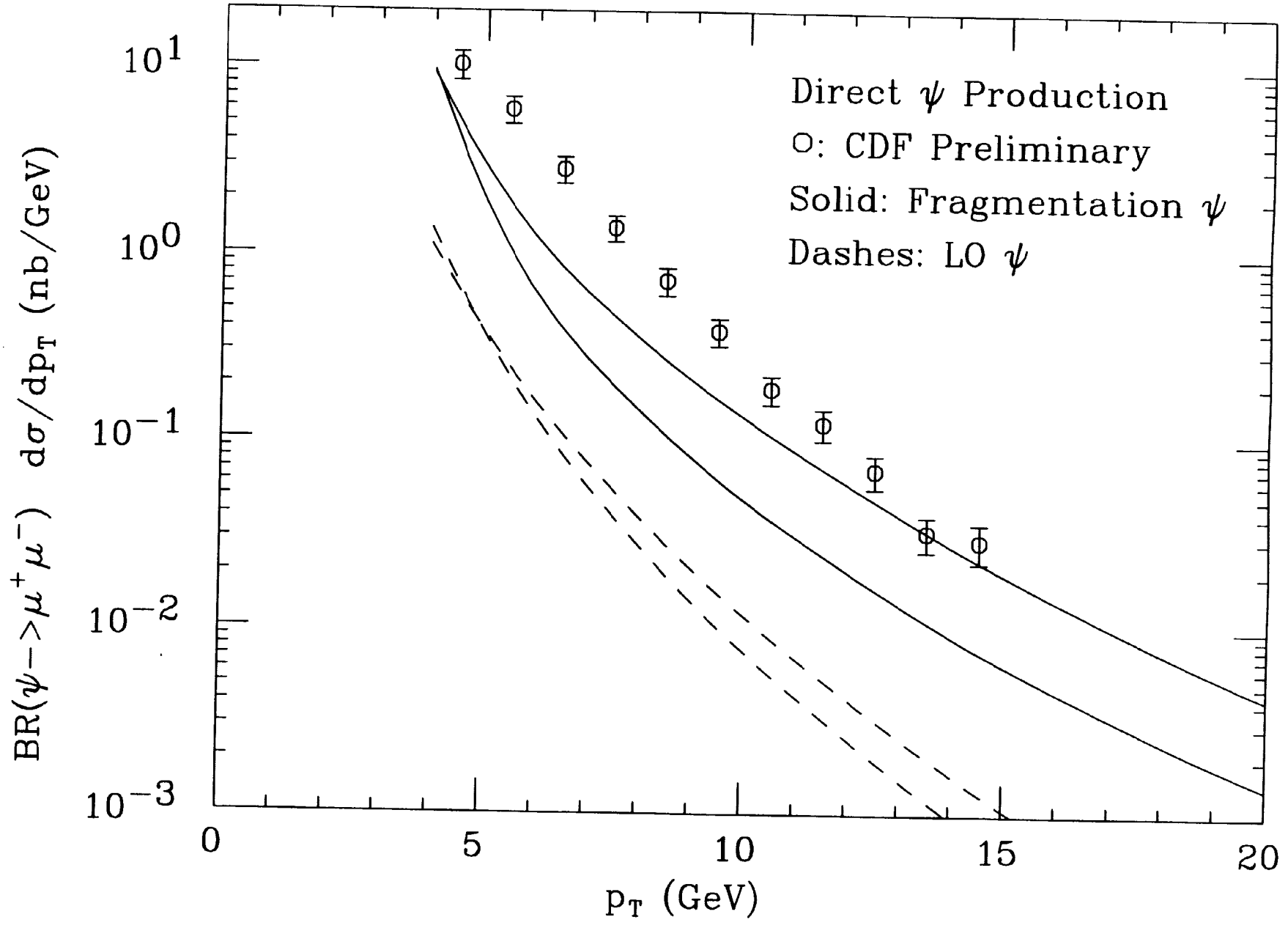
Direct ψ Production
○: CDF Preliminary
Solid: Fragmentation ψ
Dashes: LO ψ
BR(ψ−>μ⁺μ⁻) dσ/dp_T (nb/GeV)
p_T (GeV)
10^1
10^0
10^−1
10^−2
10^−3
0
5
10
15
20

Figure 2

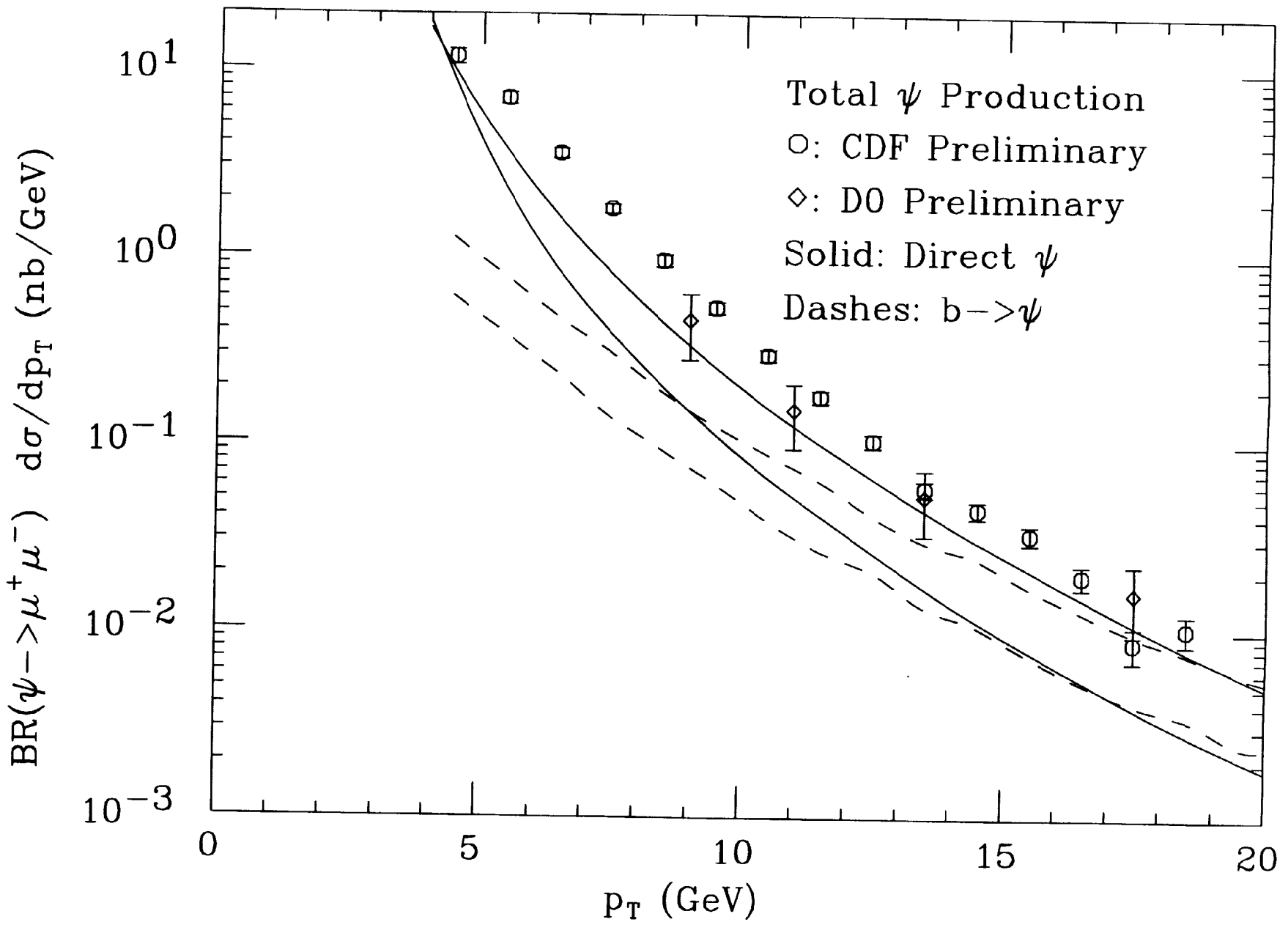
Total ψ Production
○: CDF Preliminary
◇: D0 Preliminary
Solid: Direct ψ
Dashes: b->ψ
BR(ψ->μ+μ-) dσ/dpT (nb/GeV)
pT (GeV)
10^1
10^0
10^-1
10^-2
10^-3
0
5
10
15
20

Figure 3

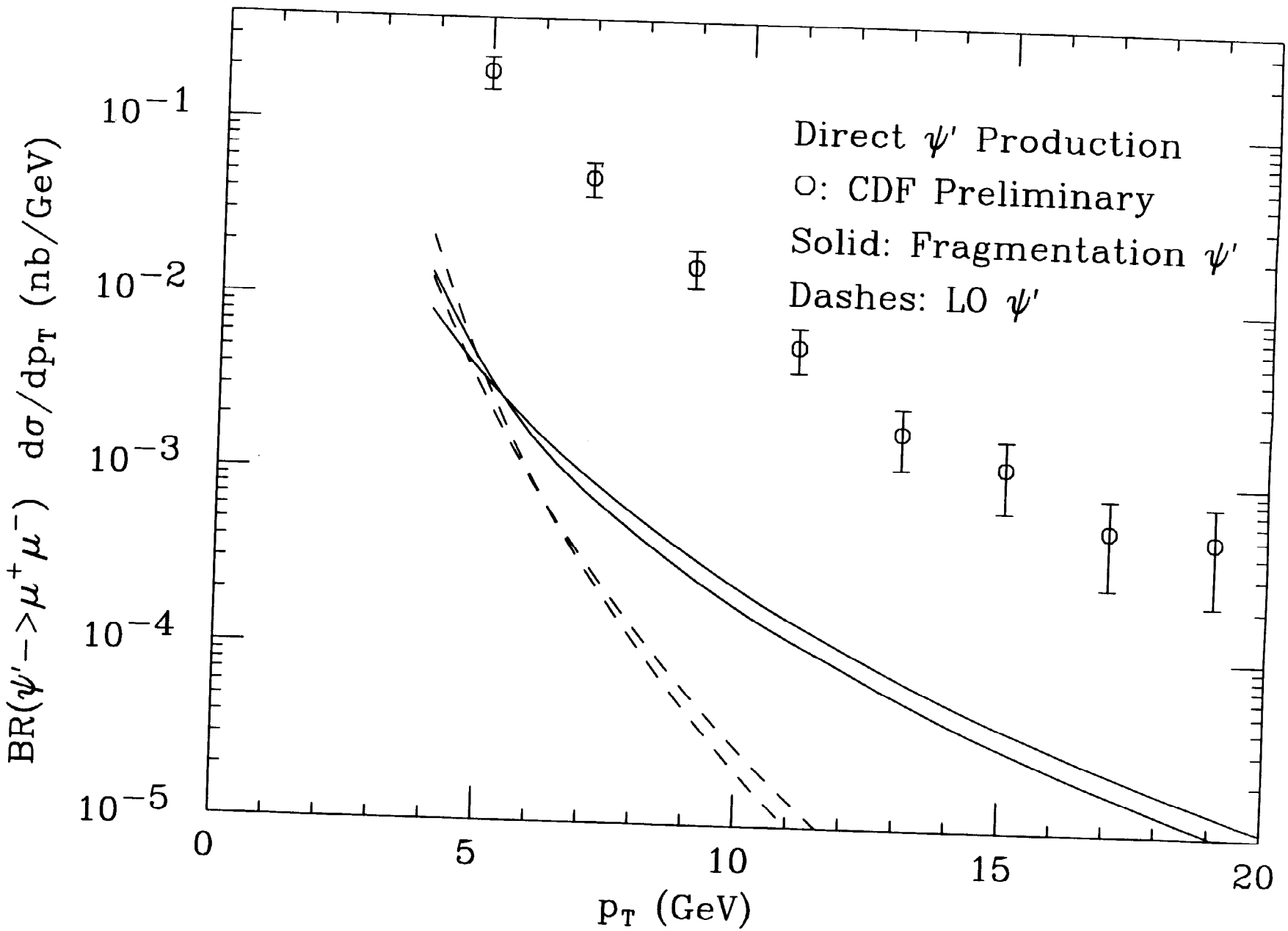
Direct ψ' Production
O: CDF Preliminary
Solid: Fragmentation ψ'
Dashes: LO ψ'
10^{-1}
10^{-2}
10^{-3}
10^{-4}
10^{-5}
$BR(\psi'->\mu^+\mu^-)$ $d\sigma/dp_T$ (nb/GeV)
0
5
10
15
20
p_T (GeV)

Figure 4